Xavier et al., J Theor Comput Sci 2014, 1:2
DOI: 10.4172/2376-130X.1000109

Journal of
Theoretical & Computational Science

Review Article Open Access

Experimental [FT-IR and FT-Raman] Analysis and Theoretical [IR, Raman, NMR and UV-Visible] Investigation on Propylbenzene

S Xavier[1,2], S Ramalingam[3]* and S Periandy[4]

[1]Department of Physics, St. Joseph College of Arts and Science, Cuddalore, Tamil Nadu, India
[2]Barathiyar University, Coimbathore, Tamilnadu, India
[3]Department of Physics, A.V.C. College, Mayiladuthurai, Tamil Nadu, India
[4]Department of Physics, Tagore Arts College, Puducherry, India

Abstract

In the present methodical study, FT-IR, FT-Raman and NMR spectra of the Propylbenzene were recorded and the fundamental vibrational frequencies were tabulated and assigned. The Gaussian hybrid computational calculations were carried out by HF and DFT (B3LYP and B3PW91) methods with 6-311+G(d,p) and 6-311++G(d,p) basis sets and the corresponding results were compared with experimental values. The change of chemical environment of present compound due to the addition of Ethyl and methyl chain was studied. Moreover, ^{13}C NMR and ^{1}H NMR were calculated by using the gauge independent atomic orbital (GIAO) method with B3LYP methods and the 6-311++G(d,p) basis set and their spectra were simulated and the chemical shifts related to TMS were compared. A study on the electronic and optical properties; absorption wavelengths, excitation energy, dipole moment and frontier molecular orbital energies, were performed by HF and DFT methods. The calculated HOMO and LUMO energies (kubo gap) were displayed in the figures which show that the occurring of charge transformation within the molecule. Besides frontier molecular orbitals (FMO), molecular electrostatic potential (MEP) was performed. NLO properties related to Polarizability and hyperpolarizability was also discussed. The local reactivity of the molecule has been studied using Fukui function.

Keywords: Propylbenzene; Gauge independent atomic orbital; Chemical shifts; FMO, Fukui function

Introduction

Propylbenzene is an organic compound that is based on the aromatic hydrocarbon with an aliphatic substitution. It is inflammable and colorless liquid, insoluble in water and less dense than water. The chemical is also flammable and incompatible with strong oxidizing agents. It is stable, but may form peroxides in storage if in contact with the air. It is important to test for the presence of peroxides before heating or distilling. Other synonyms of Propylbenzene are: n-Propylbenzene; Isocumene; Propylbenzene; 1-Phenylpropane; 1-Propylbenzene; Phenyl propane; Benzene, n-propyl. When there is contact between aromatic hydrocarbons and strong oxidizing agents it amounts to vigorous reactions sometimes amounting to explosions. They can react exothermically with bases and with diazo compounds. Substitution at the benzene nucleus occurs by halogenations (acid catalyst), nitration, sulfonation, and the Friedel-Crafts reaction.The propylbenzene is a byproduct while alkylation of benzene with propylene and it is useful a starting material for chemical synthesis [1]. Moreover, DIPB can be dehydrogenated to di-isopropenylbenzenes which can further be applied to produce plastics, elastomers and resins with valuable properties [2].

The literature survey reveals that, to the best of our knowledge, no intensive observation of spectroscopic [FT-IR and FT-Raman] and theoretical [HF/DFT] investigation has been reported so far. Therefore, the present investigation was undertaken to study the vibrational spectra, geometrical frame work review, inter and intra molecular interaction between HOMO and LUMO energy levels and first order hyperpolarizability of non linear optical (NLO) activity of the molecule.

Experimental Details

The compound Propylbenzene is purchased from Sigma–Aldrich Chemicals, USA, which is of spectroscopic grade and hence used for recording the spectra as such without any further purification. The FT-IR spectrum of the compound is recorded in Bruker IFS 66V spectrometer in the range of 4000–400 cm^{-1}. The spectral resolution is ±2 cm^{-1}. The FT-Raman spectrum of same compound is also recorded in the same instrument with FRA 106 Raman module equipped with Nd:YAG laser source operating at 1.064 μm line widths with 200 μW power. The spectra are recorded in the range of 4000–100 cm^{-1} with scanning speed of 30 $cm^{-1}min^{-1}$ of spectral width 2 cm^{-1}. The frequencies of all sharp bands are accurate to ±1 cm^{-1}.

Computational Methods

In the present work, HF and some of the hybrid methods; B3LYP and B3PW91 are carried out using the basis sets 6-31+G(d,p) and 6-311+G(d,p). All these calculations are performed using GAUSSIAN 09W [3] program package on Pentium IV processor in personal computer. In DFT methods; Becke's three parameter hybrids function combined with the Lee-Yang-Parrcorrelation function (B3LYP) [4,5], Becke's three parameter exact exchange-function (B3) [6] combined with gradient-corrected correlational functional of Lee, Yang and Parr (LYP) [7,8] and Perdew and Wang (PW91) [9,10] predict the best results for molecular geometry and vibrational frequencies for moderately larger molecules. The calculated frequencies are scaled down to give up the rational with the observed frequencies. The scaling factors

***Corresponding author:** S Ramalingam, Department of Physics, A.V.C. College, Mayiladuthurai, Tamil Nadu, India, Tel: + 04364 225367; Fax: + 04364 225367; E-mail: ramalingam.physics@gmail.com

Received December 05, 2013; **Accepted** January 15, 2014; **Published** January 22, 2014

Citation: Xavier S, Ramalingam S, Periandy S (2014) Experimental [FT-IR and FT-Raman] Analysis and Theoretical [IR, Raman, NMR and UV-Visible] Investigation on Propylbenzene. J Theor Comput Sci 1: 109. doi: 10.4172/2376-130X.1000109

are 0.959, 1.028, 1.297 for HF/6-311++G(d,p). For B3LYP/6-311+/6-311++G(d,p) basis set, the scaling factors are 0.993, 0.810/0.994,1.046, 1.09. For B3PW91/6-31+G/6-311+G(d,p) basis set, the scaling factors are 0.983, 1.04,1.08/1.01, 0.940,0.794. The optimized molecular structure of the molecule is obtained from Gaussian 09 and Gaussview program and is shown in Figure 1. The comparative optimized structural parameters such as bond length, bond angle and dihedral angle are presented in Table 1. The observed (FT-IR and FT-Raman) and calculated vibrational frequencies and vibrational assignments are submitted in Table 2. Experimental and simulated spectra of IR and Raman are presented in the Figures 2 and 3.

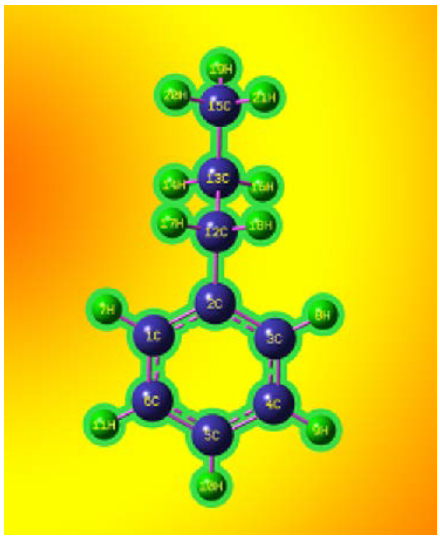

Figure 1: Molecular Structure of Propylbenzene.

The ^{1}H and ^{13}C NMR isotropic shielding are calculated with the GIAO method [11] using the optimized parameters obtained from B3LYP/6-311++G(d,p) method. ^{13}C isotropic magnetic shielding (IMS) of any X carbon atoms is made according to value ^{13}C IMS of TMS, CS_X=IMS_{TMS}-IMSx. The ^{1}H and ^{13}C isotropic chemical shifts of TMS at B3LYP methods with 6-311++G(d,p) level using the IEFPCM method in DMSO, Nitromethene and CCl4. The absolute chemical shift is found between isotropic peaks and the peaks of TMS [12]. The electronic properties; HOMO-LUMO energies, absorption wavelengths and oscillator strengths are calculated using B3LYP method of the time-dependent DFT (TD-DFT) [13,14] method in gas phase and solvent phase. Moreover, the dipole moment, nonlinear optical (NLO) properties, linear polarizabilities and first hyperpolarizabilities have also been studied. The local reactivity of the molecule has been studied using Fukui function. The condensed softness indices are found and it is used to predict both the reactive centers and possible sites of nucleophilic and electrophilic attacks.

Results and Discussion

Molecular geometry

The molecular structure of Propylbenzene belongs to CS point group symmetry. The optimized structure of the molecule is obtained from Gaussian 09 and Gauss view program [15] and is shown in Figure 1. The present molecule contains two ethyl and one methyl groups which are loaded in the left moiety. The hexagonal structure of the benzene is broken at the point of substitution due to the addition of heavy mass. It is also evident that, the bond length (C1-C2&C2-C3) at the point of substitution is 0.059Å is greater than rest of others in the

Geometrical parameter	HF/ 6-311+G(d,p)	HF/ 6-311++G (d,p)	B3LYP/ 6-311 +G (d,p)	B3LYP/ 6-311++G(d, p)	B3PW91/ 6-311+G(d,p)	B3PW91/ 6-311++G(d,p)
Bond length(Å)						
C1-C2	1.390	1.390	1.399	1.399	1.393	1.397
C1-C6	1.385	1.386	1.393	1.393	1.388	1.391
C1-H7	1.076	1.007	1.085	1.085	1.085	1.086
C2-C3	1.390	1.390	1.399	1.399	1.393	1.397
C2-C12	1.513	1.513	1.512	1.512	1.507	1.507
C3-C4	1.385	1.385	1.393	1.393	1.388	1.391
C3-H8	1.076	1.076	1.085	1.085	1.085	1.086
C4-C5	1.385	1.385	1.393	1.394	1.388	1.391
C4-H9	1.075	1.075	1.084	1.084	1.083	1.085
C5-C6	1.385	1.585	1.394	1.394	1.388	1.391
C5-H10	1.075	1.075	1.084	1.084	1.083	1.085
C6-H11	1.075	1.075	1.084	1.084	1.083	1.085
C12-C13	1.535	1.535	1.541	1.541	1.533	1.535
C12-H17	1.087	1.087	1.095	1.095	1.094	1.096
C12-H18	1.087	1.087	1.095	1.095	1.094	1.096
C13-H14	1.087	1.087	1.095	1.095	1.094	1.096
C13-C15	1.527	1.527	1.530	1.530	1.524	1.525
C13-H16	1.087	1.087	1.095	1.095	1.094	1.096
C15-H19	1.086	1.086	1.093	1.093	1.092	1.093
C15-H20	1.087	1.087	1.094	1.094	1.093	1.095
C15-H21	1.087	1.087	1.094	1.094	1.093	1.095
Bond Angle(º)						
C2-C1-C6	121.024	121.024	121.059	121.057	121.010	121.049
C2-C1-H7	119.540	119.540	119.350	119.383	119.350	119.352
C6-C1-H7	119.434	119.434	119.638	119.558	119.638	119.598

C1-C2-C3	118.182	118.181	118.247	118.145	118.247	118.158
C1-C2-C12	120.903	120.902	120.861	120.909	120.861	120.908
C3-C2-C12	120.903	120.904	120.865	120.922	120.865	120.906
C2-C3-C4	121.024	121.025	121.010	121.056	121.010	121.049
C2-C3-H8	119.540	119.539	119.351	119.386	119.351	119.352
C4-C3-H8	119.435	119.434	119.638	119.556	119.638	119.598
C3-C4-C5	120.201	120.200	120.131	120.144	120.131	120.143
C3-C4-H9	119.750	119.751	119.814	119.799	119.814	119.799
C5-C4-H9	120.047	120.048	120.053	120.055	120.053	120.055
C4-C5-C6	119.366	119.367	119.469	119.452	119.469	119.455
C4-C5-H10	120.316	120.316	120.265	120.273	120.265	120.271
C6-C5-C10	120.316	120.315	120.265	120.273	120.265	120.271
C1-C6-C5	120.201	120.200	120.131	120.143	120.131	120.143
C1-C6-H11	119.751	119.751	119.814	119.800	119.814	119.799
C5-C6-H11	120.047	120.047	120.053	120.055	120.053	120.056
C2-C12-C13	113.214	113.218	112.942	113.225	112.942	112.984
C2-C12-H17	109.311	109.310	109.552	109.515	109.552	109.546
C2-C12-H18	109.312	109.314	109.550	109.518	109.550	109.551
C13-C12-H17	109.148	109.144	109.045	108.940	109.045	109.060
C13-C12-H18	109.149	109.145	109.046	108.941	109.046	109.057
H17-C12-H18	106.483	106.486	106.495	106.474	106.495	106.426
C12-C13-H14	109.131	109.131	108.989	108.972	108.989	108.944
C12-C13-C15	112.702	112.701	112.693	112.872	112.693	112.893
C12-C13-H16	109.133	109.132	108.990	108.972	108.990	108.941
H14-C13-C15	109.686	109.689	109.921	109.842	109.9213	109.926
H14-C13-H16	106.295	109.294	106.103	106.102	106.103	105.970
C15-C13-H16	109.685	109.686	109.921	109.845	109.921	109.922
C13-C15-H19	111.070	111.065	111.376	111.269	111.376	111.322
C13-C15-H20	111.212	111.213	111.180	111.258	111.180	111.297
C13-C15-H21	111.211	111.211	111.181	111.261	111.181	111.295
H19-C15-H20	107.732	107.741	107.685	107.655	107.685	107.614
H19-C15-H21	107.732	107.741	107.684	107.655	107.684	107.613
H20-C15-H21	107.699	107.699	107.548	107.552	107.548	107.501
Dihedral Angle (º)						
C6-C1-C2-C3	-0.2286	-0.2368	-0.1521	-0.1869	-0.1521	-0.1666
C6 -C1-C2-C12	178.5556	178.5336	178.0406	178.1085	178.0406	177.9944
H7-C1-C2-C3	179.5007	179.5038	179.5501	179.5035	179.5501	179.5225
H7-C1-C2-C12	-1.7151	-1.7257	-2.2572	-2.2012	-2.2572	-2.3165
C2-C1-C6-C5	0.0739	0.0838	0.0302	0.0399	0.0302	0.0255
C2-C1-C6-H11	179.829	179.8267	179.776	179.7575	179.776	179.747
H7-C1-C6-C5	-179.6557	-179.6572	-179.6712	-179.6499	-179.6712	-179.6628
H7-C1-C6-H11	0.0994	0.0858	0.0746	0.0677	0.0746	0.0587
C1-C2-C3-C4	0.2286	0.2368	0.1525	0.1871	0.1525	0.1667
C1-C2-C3-H8	-179.4989	-179.5024	-179.5501	-179.5054	-179.5501	-179.5221
C12-C2-C3-C4	-178.5556	-178.5336	-178.0401	-178.1081	-178.0401	-177.9944
C12-C2-C3-H8	1.7169	1.7272	2.2573	2.1995	2.2573	2.3169
C1-C2-C12-C13	-89.3641	-89.3567	-89.0743	-89.0714	-89.0743	-89.0769
C1-C2-C12-H17	32.5395	32.5431	32.6862	32.7195	32.6862	32.7267
C1-C2-C12-H18	148.7309	148.7389	149.165	149.1335	149.165	149.1201
C3-C2-C12-C13	89.3802	89.3802	89.071	89.1765	89.071	89.0334
C3-C2-C12-H17	-148.7094	-148.7201	-149.1686	-149.0326	-149.1686	-149.1631
C3-C2-C12-H18	-32.518	-32.5243	-32.6898	-32.6186	-32.6898	-32.7696
C2-C3-C4-C5	-0.074	-0.0838	-0.031	-0.0404	-0.031	-0.0257
C2-C3-C4-H9	-179.8288	-179.8268	-179.7766	-179.759	-179.7766	-179.7468
H8-C3-C4-H9	179.6539	179.6557	179.6707	179.6516	179.6707	179.6622
H8-C3-C4-H9	-0.1009	-0.0873	-0.0749	-0.0671	-0.0749	-0.0589
C3-C4-C5-C6	-0.0862	-0.0751	-0.0942	-0.1109	-0.0942	-0.1189
C3-C4-C5-H10	-179.8106	-179.8093	-179.8245	-179.8336	-179.8245	-179.8281

Table 1: The optimized geometrical parameters of propylbenzene.

S. No	Symmetry Species C_s	Observed Frequency(cm^{-1})		Methods					Vibrational Assignments
		FT-IR	FT-Raman	HF	B3LYP		B3PW91		
				6-311+G (d, p)	6-311+G (d, p)	6-311++G (d, p)	6-311+G (d, p)	6-311++G (d, p)	
1	A′	3090w	-	3093	3097	3095	3090	3096	(C-H) υ
2	A′	3080m	-	3080	3084	3082	3079	3083	(C-H) υ
3	A′	-	3070m	3071	3076	3073	3070	3075	(C-H) υ
4	A′	-	3060m	3059	3063	3060	3057	3062	(C-H) υ
5	A′	-	3040s	3056	3062	3059	3056	3060	(C-H) υ
6	A′	3030s	-	2976	2997	2994	2998	3006	(C-H) υ
7	A′	-	3010w	2973	2994	2991	2993	3001	(C-H) υ
8	A′	3005w	3005w	2956	2972	2970	2973	2979	(C-H) υ
9	A′	2960s		2937	2951	2949	2954	2958	(C-H) υ
10	A′		2940s	2927	2937	2935	2935	2938	(C-H) υ
11	A′	2930s	-	2920	2931	2930	2930	2931	(C-H) υ
12	A′	-	2870m	2912	2928	2925	2927	2929	(C-H) υ
13	A′	1610w	-	1653	1596	1596	1621	1605	(C=C) υ
14	A′	1605w	1605m	1628	1578	1575	1599	1584	(C=C) υ
15	A′	1590w	1590m	1524	1513	1558	1490	1478	(C=C) υ
16	A″	1500s	-	1505	1499	1503	1461	1454	(CH3) α
17	A′	1495s	-	1491	1486	1490	1448	1443	(C-C) υ
18	A′	1455m	-	1442	1484	1442	1440	1436	(C-C) υ
19	A′	1450s	-	1436	1476	1434	1438	1430	(C-C) υ
20	A′	-	1440w	1428	1421	1429	1433	1428	(C-C) υ
21	A′	1380w	-	1374	1353	1361	1363	1354	(C-C) υ
22	A′	1340w	1340w	1352	1325	1333	1323	1330	(C-C) υ
23	A′	-	1290w	1315	1305	1312	1293	1316	(C-H) δ
24	A′	-	1280w	1277	1286	1294	1267	1306	(C-H) δ
25	A′	-	1250w	1272	1267	1275	1253	1273	(C-H) δ
26	A′	-	1200s	1221	1262	1203	1253	1262	(C-H) δ
27	A′	-	1190w	1181	1196	1193	1186	1201	(C-H) δ
28	A′	-	1180w	1170	1175	1172	1174	1188	(C-H) δ
29	A′	1160w	1160w	1150	1152	1149	1142	1157	(C-H) δ
30	A′	1105w	-	1100	1132	1129	1117	1137	(C-H) δ
31	A′	1100w	-	1106	1094	1075	1100	1069	(C-H) δ
32	A′	1095w	1095w	1077	1078	1059	1094	1057	(C-H) δ
33	A′	1050w	-	1051	1041	1023	1051	1019	(C-H) δ
34	A′	1040w	-	1032	1022	1004	1036	1007	(C-H) δ
35	A′	1030w	-	1024	1010	993	1032	1002	(C-C) δ
36	A′	-	1000s	1018	990	972	1001	968	(C-C) δ
37	A′	910w		943	974	952	997	913	(C-C) δ
38	A″	895w	-	929	956	937	979	902	(C-H) γ
39	A″	890w	890w	882	868	886	895	896	(C-H) γ
40	A″	-	865w	824	835	855	839	871	(C-H) γ
41	A″	-	840w	814	821	841	815	846	(C-H) γ
42	A″	820w	820	806	798	815	802	826	(C-H) γ
43	A″	740vs	740vs	757	770	788	771	760	(C-H) γ
44	A″	705vs	-	710	711	727	714	700	(C-H) γ
45	A″	700vs	-	682	697	713	691	682	(C-H) γ
46	A″	-	610m	664	665	649	666	655	(C-H) γ
47	A″	590s	590w	583	594	580	591	581	(C-H) γ
48	A″	570vs		550	559	546	558	547	(C-H) γ
49	A″	530vw		505	493	542	496	489	(C-H) γ
50	A′	490s	-	418	410	442	404	398	(CCC) δ
51	A′	480s	-	341	343	370	337	332	(CCC) δ
52	A′	470vw	-	305	307	330	302	299	(CCC) δ
53	A″	400 m	-	278	276	297	271	266	(CCC) γ
54	A″	370m		238	227	245	225	222	(CCC) γ
55	A″	280s	-	103	101	109	99	98	(CCC) γ
56	A″	270s	-	84	82	89	82	80	(C-C) γ
57	A″	260s	-	37	45	48	38	43	(C-C) γ

Table 2: Observed and calculated vibrational frequencies of propylbenzene using HF and DFT (B3LYP & B3PW91) at the 6-31+& 6-311+G (d, p) level.

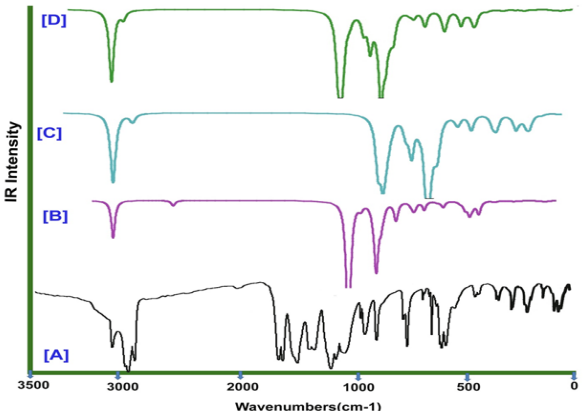

Figure 2: Experimental [A] and Calculated [B,C & D] FT-IR spectra of Propylbenzene.

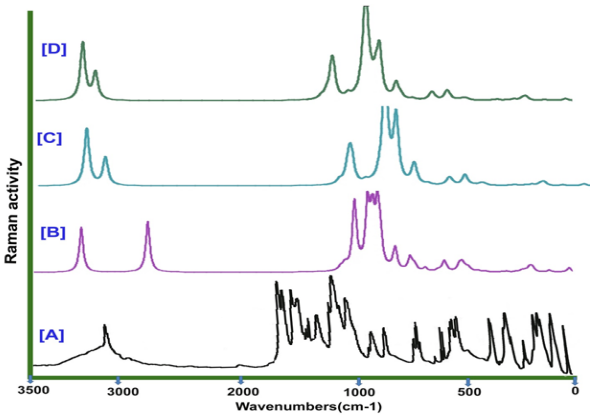

Figure 3: Experimental [A] and calculated [B,C&D] FT-Raman spectra of Propylbenzene.

ring. Consequently, the property of the same also changed with respect to the ligand (ethyl and methyl groups). The bond angle of C1-C2-C3 is 1.306º elevated than C4-C5-C6 in the ring which also conform the breaking of hexagonal shield.

The structure optimization and zero point vibrational energy of the compound in HF and DFT(B3LYP/B3PW91) with 6-311+/6-311+G(d,p) are 123.00, 115.69, 115.679, 116.943,and 115.89 Kcal/Mol, respectively.The calculated value of HF is greater than the values of DFT method because the assumption of ground state energy in HF is greater than the true energy. Though, both C loaded by CH2, the bond length values between C2-C12 and C12-C13 are differed 0.0290 Å since further weighted by CH_3 in the chain. The entire C-H bonds in the chain and methyl group having almost equal inter nuclear distance. Form the optimized molecular structure; it is observed that there is no arithmetical change in the chain. So there is no further change in geometrical property.

Vibrational assignments

In order to obtain the spectroscopic signature of the propylbenzene, the computational calculations are performed for frequency analysis. The molecule, has CS point group symmetry, consists of 21 atoms, so it has 57 normal vibrational modes. On the basis of Cs symmetry, the 57 fundamental vibrations of the molecule can be distributed as 39

S. No.	Observed frequency	Calculated frequency				
		HF	B3LYP		B3PW91	
		6-311G (d,p)	6-31G (d,p)	6-311G (d,p)	6-31G (d,p)	6-311G (d,p)
1	3090w	3347	3187	3187	3211	3198
2	3080m	3333	3174	3174	3199	3185
3	3070m	3323	3166	3165	3190	3176
4	3060m	3310	3152	3152	3176	3163
5	3040s	3307	3151	3151	3175	3161
6	3030s	3220	3084	3084	3115	3105
7	3010w	3217	3081	3081	3110	3100
8	3005w	3199	3059	3058	3089	3077
9	2960s	3178	3037	3037	3069	3055
10	2940s	3167	3023	3023	3050	3035
11	2930s	3160	3017	3017	3044	3028
12	2910m	3151	3013	3012	3041	3025
13	1610w	1789	1643	1643	1684	1658
14	1605w	1762	1622	1622	1661	1636
15	1590w	1649	1525	1525	1548	1527
16	1500s	1629	1510	1510	1518	1502
17	1495s	1614	1497	1497	1505	1491
18	1455m	1614	1495	1495	1503	1488
19	1450s	1607	1487	1487	1501	1482
20	1440w	1598	1482	1482	1496	1479
21	1380w	1537	1411	1411	1423	1403
22	1340w	1513	1382	1382	1402	1378
23	1290w	1471	1361	1361	1371	1363
24	1280w	1429	1342	1342	1343	1353
25	1250w	1423	1322	1322	1328	1319
26	1200s	1366	1316	1316	1328	1308
27	1190w	1321	1248	1248	1257	1244
28	1180w	1309	1226	1226	1244	1231
29	1160w	1287	1202	1202	1210	1199
30	1105w	1231	1181	1181	1184	1178
31	1100w	1199	1124	1124	1132	1122
32	1095w	1168	1108	1108	1126	1110
33	1050w	1139	1070	1070	1082	1070
34	1040w	1119	1050	1050	1066	1057
35	1030w	1110	1038	1038	1062	1052
36	1000s	1104	1017	1017	1030	1016
37	910w	1097	1001	996	1026	995
38	895w	1081	982	980	1007	980
39	890w	1026	929	927	949	926
40	865w	959	894	894	912	900
41	840w	947	879	879	886	874
42	820w	938	854	853	872	853
43	740vs	881	824	824	838	826
44	705vs	826	761	760	776	761
45	700vs	794	746	746	751	741
46	610m	772	712	712	724	712
47	590s	678	636	636	642	632
48	570vs	640	598	599	606	595
49	530vw	547	507	507	515	505
50	490s	452	413	414	420	411
51	480s	369	346	346	350	343
52	470vw	330	309	309	314	309
53	400 m	301	278	278	282	275
54	370m	258	229	229	234	229
55	280s	112	102	102	103	101
56	270s	91	83	83	85	83
57	260s	40	45	45	40	44

Table 3: Calculated unscaled frequencies of propyl benzene using HF/DFT (B3LYP&B3PW91) with 6-31+(d,p) and 6-311+G(d,p) basis sets.

in-plane vibrations of A′ species and 18 out of plane vibrations of A″ species, i.e., Γ_{vib} = 39 A′ + 18 A″. In the CS group symmetry of molecule is non-planar structure and has the 57 vibrational modes span in the irreducible representations.

The harmonic vibrational frequencies (unscaled and scaled) calculated at HF, B3LYP and B3PW91 levels using the triple split valence basis set along with the diffuse and polarization functions, 6-31+/6-311++G(d,p) and observed FT-IR and FT-Raman frequencies for various modes of vibrations have been presented in Tables 2 and 3. Comparison of frequencies calculated at HF andB3LYP/B3PW91 with the experimental values reveal the over estimation of the calculated vibrational modes due to the neglect of a harmonicity in real system. Inclusion of electron correlation in the density functional theory to certain extends makes the frequency values smaller in comparison with the HF frequency data. Reduction in the computed harmonic vibrations, although basis set sensitive is only marginal as observed in the DFT values using 6-311+G (d,p).

C-H Vibrations: The C–H stretching vibrations are normally observed in the region 3100–3000 cm^{-1} for aromatic benzene structure [16,17] which shows their uniqueness of the skeletal vibrations. The bands appeared at 3090, 3070, 3065, 3060 and 3040 cm^{-1} in the Propylbenzene have been assigned to C–H ring stretching vibrations. The C–H in-plane ring bending vibrations are normally occurred as a number of strong to weak intensity bands in the region 1300-1000 cm^{-1} [18]. In the present case, four C–H in-plane bendingvibrations of the present compound are identified at 1290, 1280, 1250 and 1200 cm 1. The calculated frequencies for B3LYP/6-31++G (d,p) and B3LYP/6-311++G (d, p) methods for C–H in-plane bending vibrations showed excellent agreement with recorded spectrum as well as literature data. The C–H out-of-plane bending vibrationsare normally observed in the region 1000–809 cm^{-1} [19]. The C–H out of plane bending vibrations is observed at 895, 890, 865, 840 and 820 cm^{-1}. The entire C-H stretching and bending vibrations are located at the top end of the expected region which is because of these vibrations have not affected by ethyl and methyl group in the molecule. Whereas, all the out of plane bending vibrations are suppressed to the lower end of the expected region.

Methyl groups vibrations: With the aromatic ring, for the substitution of CH3 group, the vibrational frequencies for nine fundamental vibrations such as three stretching, in plane and out of plane bending vibrations normally observed in the region of 3000- 2750 cm^{-1}, 1250-950 cm^{-1} and 950- 720 cm^{-1} [19,20], respectively.

Accordingly, the stretching vibrational peaks are observed at 3030, 3010 and 3005 cm^{-1}, in plane bending vibrational bands are found at 1180, 1160, and1105 cm^{-1} and out of plane bending signals are identified at 740, 705 and 700 cm^{-1}. All the CH_3 stretching vibrations are located in asymmetric range which shows the enhancement of CH_3 group vibrations in the present molecule. Except, two out of plane vibrations, the entire bending signals are received within the expected region. The ethyl group in the chain influences the bending vibrations of CH_3. The above assignments go along with the literature of R.N. Singh and Varsanyi [19,20].

Ethyl group vibrations: The aliphatic chain substitution CH2 ethyl group with the aromatic ring will have eight fundamental vibrations such as four stretching, in plane and out of plane bending vibrations normally found in the region of 3000 -2850, 1300-1000 cm^{-1} and 810-722 cm^{-1} [21,22], respectively. In the present study of propylbenzene the stretching vibrations are observed at 2960,2930, 2910, 2870 cm^{-1} , the in-plane bending vibrations are found at 1100, 1095, 1050, 1040 cm^{-1} and subsequently out of plane vibrations are at 610, 590, 570 and 530 cm^{-1}. All the stretching and bending vibrational bands are found within the region.

C-C vibrations: The bands due the C-C stretching vibrations are called skeletal vibrations normally observed in the region 1430 - 1650 cm^{-1} for the aromatic ring compounds [23,24]. *Socrates* [25] mentioned that, the presence of conjugate substituent suchas C=C causesstretching peaks around the region 1625-1575 cm^{-1}. As predicted in the earlier references, in this title compound,the prominent peaks are found with strong and medium intensity at 1610, 1605 and 1590 cm^{-1} due to C=C stretching vibrations. The C-C stretching vibrations are appeared at1495, 1455 and1450 cm^{-1}. The CCCin-plane and out of plane bending vibrations are appeared at 490, 480 and 470 cm^{-1} and 400, 370 and 280 cm^{-1}. Similar to the ring C-H vibrations, these skeletal CC stretching and bending vibrations are found within the expected region and also make a good agreement with literature [26].

NMR assessment: NMR spectroscopy is currently used for structure elucidation of complex molecules. The combined use of experimental and computationaltools offers a powerful gadget to interpret and predict the structure of bulky molecules. The optimized structure of Propylbenzene is used to calculate the NMR spectra at B3LYP method with 6-311++G(d,p) level using the GIAO method and the chemical shifts of the compound are reported in ppm relative to TMS for ^{1}H and ^{13}C NMR spectra which are presented in Table 4. The corresponding spectra are shown in Figure 4.

In view of the range of ^{13}C NMR chemical shifts for similar organic molecules usually is >100 ppm [27,28] the accuracy ensures reliable interpretation of spectroscopic parameters. In the present work, 13C NMR chemical shifts of some carbons in the chain are >100 ppm, as they would be expected in Table 5. In the case of Propylbenzene, the chemical shift of C1, C3, C3,C4, C5 and C6 are 81.21, 77.35, 86.13, 78.60, and 85.31 ppm, respectively. The shift is higher in C2, C12, C13 and C15 than rest of others.

The C3 in the chain has more shifted than other due to the delocalization of σ and π electrons. The shift of the entire carbons of the ring is found increased when going from gas to solvent due to the solvent effect. The shift values of carbons in DMSO phase are greater than Chloroform phase. The chemical shift values of oxygen have not changed due to the solvent effect. The experimental and theoretical ^{1}H and ^{13}C NMR chemical shift of Propylbenzene are presented in Table 5. This effect of isolation is the main cause to change the chemical property from benzene to Propylbenzene.

Optical properties (HOMO-LUMO analysis)

The UV and visible spectroscopy is used to detect the presence of chromophores in the molecule and whether the compound has NLO properties or not. The calculations of the electronic structure of Propylbenzene are optimized in singlet state. The low energy electronic excited states of the molecule are calculated at the B3LYP/6-311++G(d,p) level using the TD-DFT approach on the previously optimized ground-state geometry of the molecule. The calculations are performed for Propylbenzenein gasphase and with the solvent of DMSO, CCl4, and Nitromethene. The calculated excitation energies, oscillator strength (*f*) and wavelength (λ) and spectral assignments are given in Table 6.

TD-DFT calculations predict three transitions in the quartz ultraviolet region. In the case of gas phase, the strong transition is at 234.96, 210.53 and 205.88nm with an oscillator strength f=0.0048,

Atom position	Gas			Solvent					
				Chloroform			DMSO		
	B3LYP/6-311+G(d,p) (ppm)	B3LYP/6-311+G (2d,p) GIAO (ppm)	Shift (ppm)	B3LYP/6-311+G(d,p) (ppm)	B3LYP/6-311+G(2d,p) GIAO (ppm)	Shift (ppm)	B3LYP/6-311+G(d,p) (ppm)	B3LYP/6-311+G(2d,p) GIAO (ppm)	Shift (ppm)
C1	50.6257	131.84	81.2143	50.6257	131.84	81.2143	50.2521	132.214	81.9619
C2	35.1536	147.312	112.1584	35.1536	147.312	112.1584	33.6205	148.845	115.2245
C3	52.5577	129.908	77.3503	52.5577	129.908	77.3503	52.2505	130.215	77.9645
C4	48.1658	134.3	86.1342	48.1658	134.3	86.1342	48.155	134.31	86.155
C5	51.9287	130.537	78.6083	51.9287	130.53	78.6013	52.2318	130.234	78.0022
C6	48.5706	133.89	85.3194	48.5706	133.89	85.3194	48.5497	133.916	85.3663
C12	142.636	39.8297	102.8063	142.636	39.8297	102.8063	142.899	39.5661	103.3329
C13	167.62	14.846	152.774	167.62	14.846	152.774	167.836	14.6298	153.2062
C15	169.06	13.4059	155.6541	169.06	13.4059	155.6541	169.613	12.8531	156.7599
7H	24.3718	7.5103	16.8615	24.3718	7.5103	16.8615	24.1899	7.6922	16.4977
8H	24.1444	7.7377	16.4067	24.1444	7.7377	16.4067	23.9782	7.9039	16.0743
9H	24.286	7.5961	16.6899	24.286	7.5961	16.6899	24.1354	7.7467	16.3887
10H	24.4747	7.4074	17.0673	24.4747	7.4074	17.0673	24.3433	7.5388	16.8045
11H	24.2974	7.5847	16.7127	24.2974	7.5847	16.7127	24.1446	7.7375	16.4071
14H	30.66	1.2221	29.4379	30.66	1.2221	29.4379	30.628	1.2541	29.3739
16H	31.0626	0.8195	30.2431	31.0626	0.8195	30.2431	31.0074	0.874	30.1334
17H	30.2216	1.6605	28.5611	30.2216	1.6605	28.5611	30.1511	1.731	28.4201
18H	29.2452	2.6369	26.6083	29.2452	2.6369	26.6083	29.191	2.6911	26.4999
19H	31.0626	0.8219	30.2407	31.0602	0.8219	30.2383	31.064	0.8181	30.2459
20H	32.0056	-0.1235	32.1291	32.0056	-0.1235	32.1291	31.9903	-0.1082	32.0985
21H	31.1101	0.772	30.3381	31.1101	0.772	30.3381	31.0941	0.788	30.3061

Table 4: Experimental and calculated 1H and 13C NMR chemical shifts (ppm) of propylbenzene.

λ(nm)	E (eV)	(f)	Major contribution	Assignment	Region	Bands
Gas						
234.96	5.276	0.0048	H→L (92%)	n→π*	Quartz UV	R-band (German, radikalartig)
210.53	5.889	0.0162	H→L (89%)	n→π*	Quartz UV	
205.88	6.0220	0.0015	H→L (86%)	n→π*	Quartz UV	
DMSO						
234.72	5.282	0.0082	H→L-1 (90%)	n→π*	Quartz UV	R-band (German, radikalartig)
210.99	5.876	0.0258	H→L-1 (90%)	n→π*	Quartz UV	
201.57	6.150	0.0022	H→L-1 (87%)	n→π*	Quartz UV	
			H+1→L-1 (83%)	σ→σ*	Quartz UV	
CCl_4						
235.13	5.273	0.0082	H→L-1 (86%)	n→π*	Quartz UV	R-band (German, radikalartig)
211.41	5.864	0.0252	H→L-1 (85%)	n→π*	Quartz UV	
204.13	6.0736	0.0020	H→L-1 (78%)	n→π*	Quartz UV	
			H+1→L-1(77%)	σ→σ*	Quartz UV	
Nitro methyl						
234.70	5.282	0.0080	H+1→L (86%)	n→π*	Quartz UV	R-band (German, radikalartig)
210.93	5.878	0.0252	H+1→L-1 (85%)	n→π*	Quartz UV	
201.59	6.150	0.002	H→L-1 (78%)	n→π*	Quartz UV	
			H+1→L-1(74%)	σ→σ*	Quartz UV	

Table 5: Theoretical electronic absorption spectra of propylbenzene (absorption wavelength *λ* (nm), excitation energies *E* (eV) and oscillator strengths (*f*)) obtained using the TD-DFT/B3LYP/6-311++G(d,p) method.

0.0162, 0.0015 with 5.2767 eV energy gap. The transition is n→π* in visible and quartz ultraviolet region. The designation of the band is R-band(German, radikalartig) which is attributed to above said transition of prophyl groups. They are characterizes by low molar absorptivities (ξ_{max}<100) and undergo hypsochromic shift with an increase in solvent polarity. The simulated UV-Visible spectra in gas and solvent phase of Propylbenzene are shown in Figure 5.

In the case of DMSO solvent, strong transitions are 234.72, 210.99, 201.57 nm with an oscillator strength f=0.0082, 0.0258, 0.0022 nm with maximum energy gap 6.1509 eV.They are assigned to n → π* and σ→ σ*transitions and belongs to quartz ultraviolet region. This shows that, from gas to solvent, the transitions moved from visible to quartz ultraviolet region. This view indicates that, the Propylbenzene molecule having crystal property and thus, it is capable of having rich NLO properties. In addition to that, the calculated optical band gap 5.111 eV which ensure that the present compound has NLO properties. In view of calculated absorption spectra, the maximum absorption wavelength corresponds to the electronic transition from the HOMO to LUMO with maximum contribution.

The chemical hardness and potential, electronegativity and Electrophilicity index are calculated and their values are shown in Table 7. The chemical hardness is a good indicator of the chemical stability. The chemical hardness is decreased slightly (1.72-3.01) in going from Gas to solvent. Hence, the present compound has much chemical

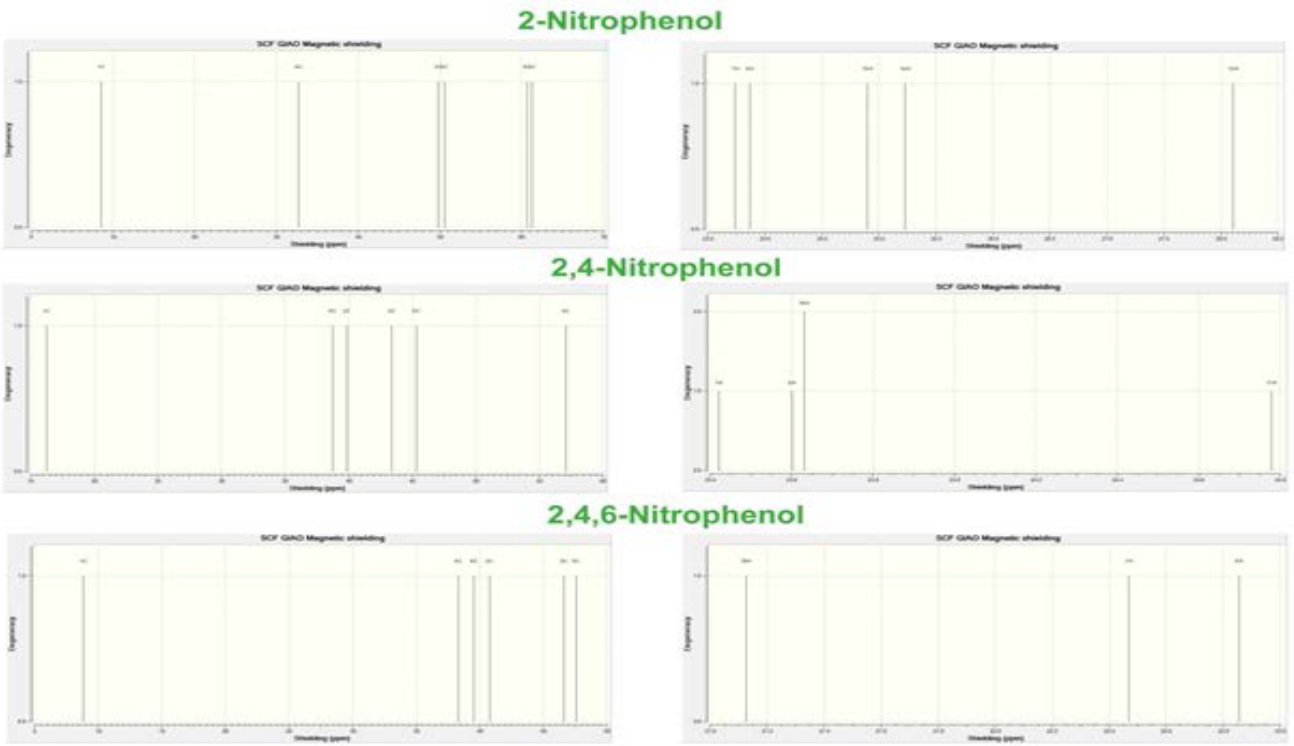

Figure 4: ^{1}H and ^{13}C NMR spectra of Propylbenzene in Gas and Solvant phase.

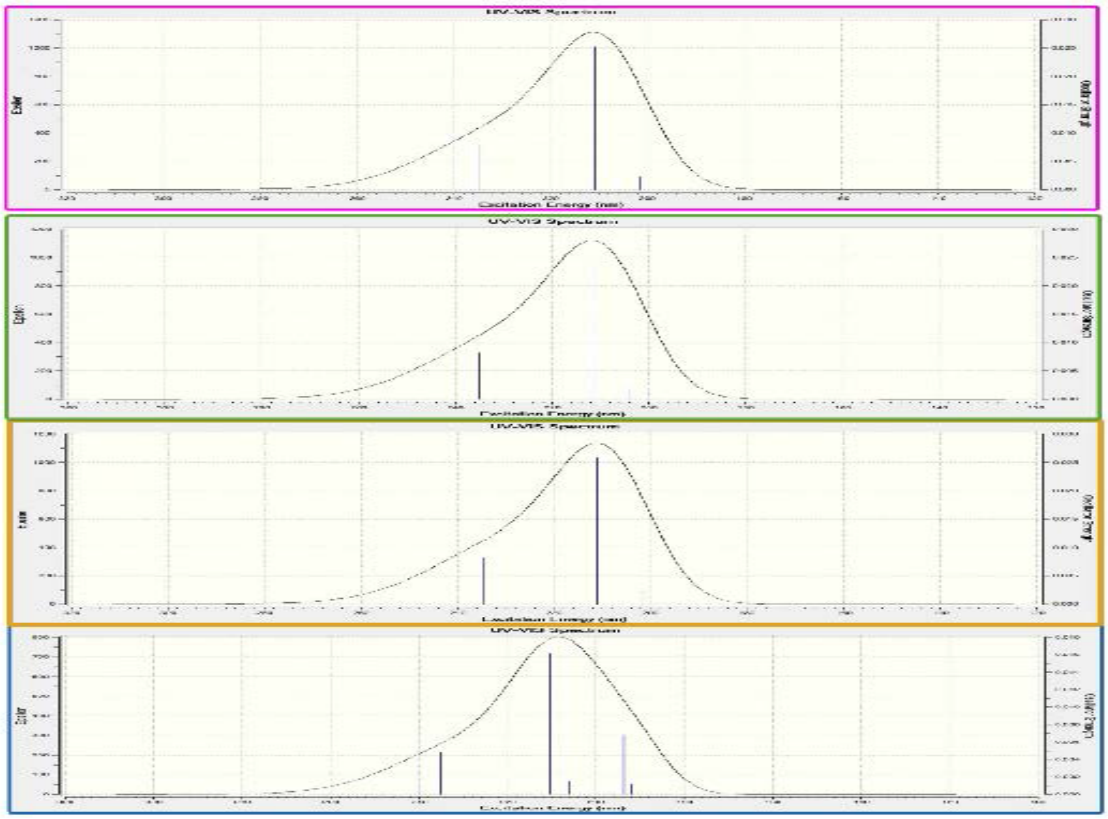

Figure 5: UV Visible spectra of Propylbenzene in Gas and Solvant Phase.

stability. Similarly, the electronegativity is increased from 3.45 upto 3.36, from Gas to solvent, if the value is greater than 1.7; the property of bond is changed from covalent to ionic. Accordingly, the bonds in the compound converted from covalent to ionic and are independent of solvent. Electrophilicity index is the measure of energy lowering due to maximal electron flow between donor [HOMO] and acceptor [LUMO]. From the Table 7, it is found that the Electrophilicity index of Propylbenzene is 3.45 in gas and 3.36 in solvent, which is moderate and this value ensure that the strong energy transformation between HOMO and LUMO.The dipole moment in a molecule is another important electronic property. Whenever the molecule has larger the dipole moment, the intermolecular interactions are very strong. The calculated dipole moment value for the title compound is 12.24 Debye in gas and 15.75 in solvent. It is too high which shows that; the Propylbenzene molecule has strong intermolecular interactions.

Global softness and local region-selectivity

Molecular charge distribution, molecular orbital surfaces and HOMO and LUMO energies have been used as reactivity descriptors in DFT study. The energy gap between the HOMO and LUMO orbital have been found to be adequate to study the stability and chemical reactivity of great variety of molecular system and is an important stability index. Besides the traditional reactivity descriptors there are a set of chemical reactivity descriptors which can be derived from DFT, such as global hardness (η), global softness, local softness (S), Fukui function (f) and global and local electrophilicity indexes (ω) [29-39]. These quantities are often defined by the Koopman's theorem [40,41].

Electronegativity (χ) is the measure of the power of an electron or group of atoms to attract electrons towards itself [42] and according to Koopman's theorem; it can be estimated by using the following equation:

$$\chi = -\frac{1}{2}\left(E_{Homo} + E_{Lumo}\right) \quad (1)$$

Where E_{Homo} is the energies of the highest occupied molecular orbital (HOMO) and E_{Lumo} is the energy of the lowest unoccupied molecular orbital (LUMO).Global hardness (η) measures the resistance of an atom to a charge transfer [41] and it is estimated using the equation:

$$\eta = -\frac{1}{2}\left(E_{Homo} + E_{Lumo}\right) \quad (2)$$

Global softness (S) describes the capacity of an atom or group of atoms to receive electrons [43] and it is estimated by using the equation:

$$S = \frac{1}{\eta} = -2\left(E_{Homo} - E_{Lumo}\right) \quad (3)$$

Where, η is the global hardness values. Global electrophilicity index (ω) is estimated by using the electronegativity and chemical hardness parameters through the equation:

$$\omega = \frac{\chi^2}{2\eta} \quad (4)$$

A high value of electrophilicity describes a good electrophile while a small value of electrophilicity describes a good nucleophile.

Fukui indices are a measurement of the chemical reactivity, as well as an indicator of the reactive regions and the nucleophilic and electrophilic behaviors of the molecule. The regions of a molecule where the Fukui function is large are chemically softer than the regions where the Fukui function is small, and by invoking HSAB principle in a local sense, one may establish the behavior of different sites with respect to hard or soft reagents. Condensed to atom Fukui function is reactive descriptor to identify nucleophilic and electrophilic attack site in candidate molecules, perhaps it is also used to recognize the electron acceptor center and donor centers. fk+ for any given site is positive then it is a preferred site for nucleophilic attack, on the contrary negative value implies electrophilic attack.

The Fukui function is defined as [44,45]:

$$f(r) = \left[\frac{\partial\rho(r)}{\delta N}\right]_{v(r)} \quad (5)$$

Where ρ(r) is the electron density and N

$$N = \int \rho(r)\, dr \quad (6)$$

N is the number of electrons and r is the external potential exerted by the nucleus.

Phenyl ring gets activated at ortho and para positions as there are electron releasing substituent such as -OH, -NH_2, -OR, R, etc. Propyl substituent in fact is an electron releasing substituent, consequently promotes the ortho and para positions for electrophilic attack a common reactivity trend observed in phenyl compounds. Local reactivity descriptors such as fk+,fk-, Δf, Δω for the different sites of phenyl ring are in conformity with the observed reactivity trend of the candidate molecule.

fk+,fk-, Δf, Δω unambiguously reveal the nucleophilic attack to be in the decreasing sequence asC6>C4 >C2 and that of electrophilic attack is found to be in the order C1>C3>C5 in the phenyl ring. This trend for attack of electrophile is in conformity with that of ΔS and Δω. The ortho and para positions show the tendency for attack of electrophile which is indeed a common trend observed in alkyl substituted phenyl ring compounds.

Molecular electrostatic potential (MEP) maps

The molecular electrical potential surfaces illustrate the charge distributions of molecules three dimensionally. This map allows us to visualize variably charged regions of a molecule. Knowledge of the charge distributions can be used to determine how molecules interact with one another and it is also be used to determine the nature of the chemical bond.Molecular electrostatic potential is calculated at the B3LYP/6-311+G(d,p) optimized geometry [46,47]. There is a great deal of intermediary potential energy, the non red or blue regions indicate that the electro negativity difference is not very great. In a molecule with a great electro negativity difference, charge is very polarized, and there are significant differences in electron density in different regions of the molecule. This great electro negativity difference leads to regions that are almost entirely red and almost entirely blue [48]. Greater regions of intermediary potential, yellow and green, and smaller or no regions of extreme potential, red and blue, are key indicators of a smaller electronegativity.

The color code of these maps is in the range between -6.15 a.u. (Deepest red) to 6.15 a.u. (deepest blue) in compound. The positive (blue) regions of MEP are related to electrophilic reactivity and the negative (green) regions to nucleophilic reactivity shown in Figure 6. From the MEP map of the candidate molecule the red regions of the molecule found to be ready for electrophilic attack, and especially in the phenyl ring the atoms are clouded with red colour. From the findings of the Fukui local reactivity descriptor the atoms C1, C3 and C5 are nucleophile ready for electrophilic attack and atoms C2, C4 and C6 are the regions for nucleophilic attack. Molecular electrostatic potential map can be confirmed with the finding of the Fukui descriptors.

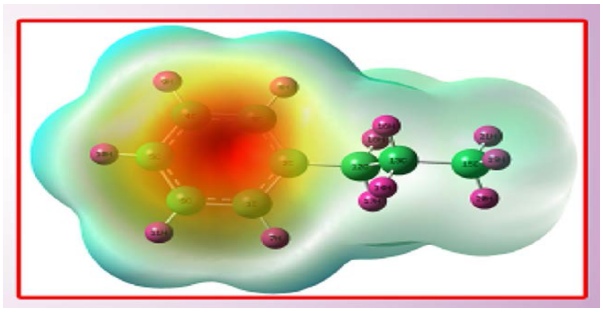

Figure 6: MEP map of propylbenzene.

f+ = (q+1)-q	f-=q-(q-1)	Δf=(f+)-(f-)	ΔS =Δfσ$_{gs}$	Δω=Δfω$_{gei}$
-0.0990	5.5674	-5.6665	-64.971	-0.3539
0.10410	-1.0720	1.1761	13.4852	0.0734
-0.0989	5.57436	-5.6732	-65.049	-0.3544
-0.0488	-3.9275	3.8786	44.472	0.2422
-0.1308	0.4939	-0.6248	-7.1641	-0.0390
-0.0487	-3.9281	3.8793	44.480	0.2423
-0.0636	-3.1527	3.0890	35.419	0.1929
0.03984	-0.0434	0.0832	0.9542	0.0051
-1.1396	-0.7127	-0.4268	-4.8945	-0.0266

ΔS = local softness, σ$_{gs}$- global softeness; -Δω local electophilic index, ω$_{gei}$- global electrophilic index

Table 6: Fukui function and global and local softness, and electrophilicity index of propylbenzene.

Parameters	Gas	CCl4	Nitromethene	DMSO
EHOMO (eV)	-6.63169	-5.25427	-6.824886218	-6.82679
ELUMO (eV)	-0.39865	-0.4928	-0.572527435	-0.57443
ΔEHOMO-LUMO gap (eV)	-6.23304	-4.76147	-6.252358783	-6.25236
Electronegativity (χ)	3.5151	2.380736	3.126179391	3.126179
Chemical hardness (η)	-3.11652	-2.38074	-3.126179391	-3.12618
Global softness (σ)	-0.32087	-0.42004	-0.319879276	-0.31988
Electrophilicity index (ω)	-1.98346	-1.19037	-1.563089696	-1.56309
Dipole moment (μ)	15.44518	17.7527	21.17546183	20.47384

Table 7: HOMO, LUMO, Kubo gap, global electronegativity, global hardness and softness, global electrophilicity index of propylbenzene.

Polarizability and first order hyperpolarizability calculations

In order to investigate the relationships among molecular structures and non-linear optic properties (NLO), the polarizabilities and first order hyperpolarizabilities of the Propylbenzene compound was calculated using DFT-B3LYP method and 6-311+G(d,p) basis set, based on the finite-field approach.

The Polarizability and hyperpolarizability tensors (Table 8) (α_{xx}, α_{xy}, α_{yy}, α_{xz}, α_{yz}, α_{zz} *and* β_{xxx}, β_{xxy}, β_{xyy}, β_{yyy}, β_{xxz}, β_{xyz}, β_{yyz}, β_{xzz}, β_{yzz}, β_{zzz}) can be obtained by a frequency job output file of Gaussian. However, α and β values of Gaussian output are in atomic units (a.u.). So they have been converted into electronic units (esu) (α; 1 a.u.=0.1482×10^{-24}esu, β; 1 a.u.=8.6393×10^{-33} esu). The calculations of the total molecular dipole moment (μ), linear polarizability (α) and first-order hyperpolarizability (β) from the Gaussian output have been explained in detail previously [49,50] and DFT has been extensively used as an effective method to investigate the organic NLO materials [51-55].

$$\alpha_{tot} = \frac{1}{3}\left(\alpha_{xx} + \alpha_{yy} + \alpha_{zz}\right) \quad (7)$$

$$\Delta\alpha = \frac{1}{\sqrt{2}}\left[\left(\alpha_{xx} - \alpha_{yy}\right)^2 + \left(\alpha_{yy} - \alpha_{zz}\right)^2 + \left(\alpha_{zz} - \alpha_{xx}\right)^2 + 6\alpha_{xz}^2 + 6\alpha_{xy}^2 + 6\alpha_{yz}^2\right]^{\frac{1}{2}} \quad (8)$$

$$\langle\beta\rangle = \left[\left(\beta_{xxx} + \beta_{xyy} + \beta_{xzz}\right)^2 + \left(\beta_{yyy} + \beta_{yzz} + \beta_{yxx}\right)^2 + \left(\beta_{zzz} + \beta_{zxx} + \beta_{zyy}\right)^2\right]^{\frac{1}{2}} \quad (9)$$

In Table 7, the calculated parameters described above and electronic dipole moment {$\mu_i (i$ = x, y, z) and total dipole moment μ_{tot}} for title compound are listed. The total dipole moment was calculated using the following equation [56].

$$\mu_{tot} = \left(\mu_x^2 + \mu_y^2 + \mu_z^2\right)^{\frac{1}{2}} \quad (10)$$

It is well known that, molecule with high values of dipole moment, molecular Polarizability, and first hyperpolarizability having more active NLO properties. The first hyperpolarizability (β) and the component of hyperpolarizability β_x, β_y and β_z of Propylbenzene along with related properties (μ_0, α_{total}, and Δα) are reported in Table 6. The calculated value of dipole moment is found to be 0.16111 Debye. The highest value of dipole moment is observed for component μ_X. In this direction, this value is equal to 0.0731 D. The lowest value of the dipole moment of the molecule compound is μ_Y component (-0.0696 D). The calculated average Polarizability and anisotropy of the Polarizability is -55.2077×10^{-24} esu and 6.6956×10^{-24} esu, respectively. The magnitude of the molecular hyperpolarizability β, is one of important key factors in a NLO system. The B3LYP/6-311+G(d,p) calculated first hyperpolarizability value (β) is 2.9780×10^{-30} esu. From the above results, it is observed that, the molecular Polarizability and hyperpolarizability of the title compound in all coordinates are active.

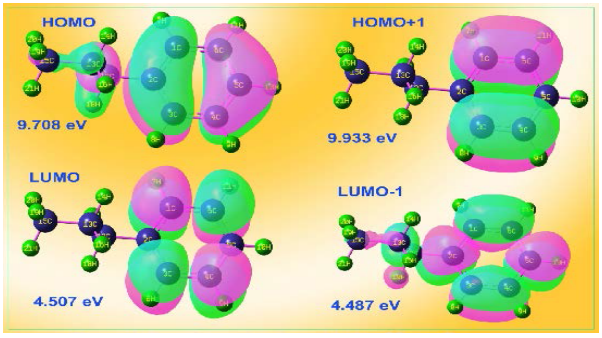

Figure 7: Frontier Molecular Orbitals of Propylbenzene.

Parameter	a.u.	Parameter	a.u.
α_{xx}	- 53.3963	β_{xxx}	13.79
α_{xy}	-0.2807	β_{xxy}	0.9912
α_{yy}	-52.6869	β_{xyy}	3.7575
α_{xz}	-0.9506	β_{yyy}	0.8982
α_{yz}	-0.2339	β_{xxz}	0.4223
α_{zz}	-59.5384	β_{xyz}	0.6611
α_{ot}	-55.2072	β_{yyz}	-0.7173
$\Delta\alpha$	6.695	β_{xzz}	-9.9781
μ_x	-0.5586	β_{yzz}	-1.0315
μ^y	- 0.0696	β_{zzz}	1.4772
μ_z	0.0731	β_{tot}	2.940
μ^{ot}	0.1611		

Table 8: The electronic dipole moment (μ) (Debye), polarizability (α) and first hyperpolarizability (β) of propylbenzene.

So that, the Propylbenzene can be used to prepare NLO crystals and those crystal is able to produce second order harmonic waves.

Conclusion

In the present investigation, FT-IR, FT-Raman and ^{13}C NMR and ^{1}H NMR spectra of the Propylbenzene were recorded and the observed vibrational frequencies were assigned depending upon their expected region. The chronological change of finger print and group frequency region of the amino acid with respect to the functional group has also monitored. The change of geometrical parameters along with the substitutions was deeply analyzed. The simulated ^{13}C NMR and ^{1}H NMR were compared with the recorded spectrum and the chemical shifts related to TMS were studied. The change of chemical properties of the molecule by the substitutions has been analysed. The electrical and optical properties of the Propylbenzene were profoundly investigated using frontier molecular orbital (Figure 7). From the UV-Visible spectra, it was found that the present compound was optically active and posses NLO properties. The molecular electrostatic potential (MEP) map was performed and from which the change the chemical properties of the compound was also discussed. The possible sites of nucleophilic and electrophilic attacks in the molecule were determined through local reactivity and Fukui condensed softness indices.

References

1. Tsai TC, Liu SB, Wang I (1999) Disproportionation and transalkylation of alkylbenzenes over zeolite catalysts. Applied Catalysis A: General 181: 355-398.
2. Ostrowski S, Jan CZ, Dobrowolski, Jamro'z MH, Brzozowski R (2004) Equilibrium mixture of the diisopropylbenzenes: a DFT study. Catalysis Communications 5: 733-737.
3. Hawley GG, Lewis RJ(Sr.) (1993) Hawley's Condensed Chemical Dictionary. (12th edn) Van NostrandRheinhold, 115 Fifth Avenue, New York, USA.
4. Hartley, Kidd D, Hamish (1991) The Agrochemicals Handbook. Royal Society of Chemistry: Nottingham, England.
5. Gerhartz W (1985) Ullmann's Encyclopedia of Industrial Chemistry. (5th edn) Deerfield Beach, FL: VCH Publishers.
6. Marchewka MK, Pietraszko A (2008) Crystal structure and vibrational spectra of piperaziniumbis(4-hydroxybenzenesulphonate) molecular-ionic crystal. Spectrochim Acta A Mol Biomol Spectrosc 69: 312-318.
7. Ivan SL, Gustavo ES (2008) The screened hybrid density functional study of metallic thorium carbide. Chem Phys Lett 460: 137-140.
8. Pejov L, Ristova M, Soptrajanov B (2011) Quantum chemical study of p-toluenesulfonic acid, p-toluenesulfonate anion and the water-p-toluenesulfonic acid complex. Comparison with experimental spectroscopic data. SpectrochimActa A MolBiomolSpectrosc 79: 27-34.
9. M.J. Frisch (2009) Gaussian 09, Revision A.1, Gaussian, Inc., Wallingford CT.
10. Zhengyu Z, Dongmei D, Xinga Y, Khan SUM (2000) Calculation of the energy of activation in the electron transfer reaction not involving the bond rupture at the electrode. Journal of Molecular Structure (Theochem) 505: 247-252.
11. Zhengyu Z, Aiping F, Dongmei D (2000) Studies on density functional theory for the electron-transfer reaction mechanism between M-C6H6 and M+-C6H6 complexes in the gas phase. Journal of Quantum Chemistry 78: 186-189.
12. Becke AD (1988) Density-functional exchange-energy approximation with correct asymptotic behavior. Phys Rev A 38: 3098-3100.
13. Lee C, Yang W, Parr RG (1988) Development of the Colle-Salvetti correlation-energy formula into a functional of the electron density. Phys Rev B Condens Matter 37: 785-789.
14. Becke AD (1993) Density-functional thermochemistry. III. The role of exact exchange. Journal of Chemical Physics 98: 5648-5652.
15. Peesole RL, Shield LD, McWilliam IC (1976) Modern Methods of Chemical Analysis, Wiley, New York, USA.
16. Sharma YR (1994) Elementary Organic Spectroscopy, Principles and Chemical Applications: 92-93, S.Chande& Company Ltd., New Delhi, India.
17. Kalsi PS (2004) Spectroscopy of Organic Compounds, (6thedn) Wiley Eastern Limited, New Delhi, India.
18. Dwivedi CPD, Sharma SN (1973) Indian Journal of Pure and Applied Physics 11: 447.
19. Singh RN, Prasad SC (1974) Vibrational spectra of isomeric bromoxylenes. Spectrochimica Acta A 34: 39.
20. Varsanyi G (1973) Assignments for Vibrational Spectra of Seven Hundred Benzene Derivatives. AkademiaiKiadó, Budapest.
21. Colthup NB, Palay LH, Wiberley SE (1990) Introduction to infrared and Raman Spectroscopy, Academic press, INC, San Diego, USA.
22. Dollich FR, Fatelay WG, Bantely FF (1974) Characteristics of Raman frequencies on organic compounds. Willey, New York, USA.
23. Silverstein M, Clayton Basseler G, Morrill C(1991) Spectrometric identification of organic Compounds, John Wiley, New York, USA.
24. Brian Smith C (1999) Infrared Spectral Interpretation, CRC Press, New York, USA.
25. Socrates G (2000) Infrared and Raman Characteristics Group Frequencies, Wiley, New York, USA.
26. Altun K, Gölcük K, Kumru M (2003) Theoretical and experimental studies of the vibrational spectra of m-methylaniline. Journal of Molecular structure (Theochem) 625: 17-20.
27. Vander Maas JH and Lutz ETG (1974) Structural information from OH stretching frequencies monohydric saturated alcohols. Spectrochimica Acta 30A: 2005-2019
28. Ahmad S, Mathew S, Verma PK (1992) Indian Journal of Pure and Applied Physics 30: 764-770.
29. Parr RG, Yang W, (1989) Density Functional Theory of Atoms and Molecules, Oxford University Press, New York, USA.
30. Geerlings P, De Proft F, Langenaekar W (1999) Density Functional Theory: A Source of Chemical Concepts and a Cost - Effective Methodology for Their Calculation, Advances Quantum Chemistry 33: 303.
31. Hohenberg K, Kohn W (1964) Inhomogeneous Electron Gas. Phys Rev 136: B864-B871.
32. Pearson RG (1963) Hard and Soft Acids and Bases. J Am Chem Soc 85: 3533.
33. Parr RG, Pearson RG (1983) Absolute hardness: companion parameter to absolute electronegativity. J Am Chem Soc 105: 7512.
34. Parr RG, Donnelly RA, Levy M, Palke WE (1978) Electronegativity: The density functional viewpoint. J Chem Phys 68: 3801.
35. Pearson RG (1985) Absolute electronegativity and absolute hardness of Lewis acids and bases. J Am Chem Soc 107: 6801.
36. Parr RG, Yang W (1984) Density functional approach to the frontier-electron theory of chemical reactivity. J Am Chem Soc 106: 4049.
37. Parr RG, László v Szentpály, Liu S (1999) Electrophilicity Index. J Am Chem Soc 121: 1922.
38. Pérez P, Toro-Labbé A, Aizman A, Contreras R (2002) Comparison between experimental and theoretical scales of electrophilicity in benzhydrylcations. J Org Chem 67: 4747-4752.
39. Yang W, Mortier WJ (1986) The use of global and local molecular parameters for the analysis of the gas-phase basicity of amines. J Am ChemSoc 108: 5708-5711.
40. Geerlings P, De Proft F, Langenaeker W (2003) Conceptual density functional theory. Chem Rev 103: 1793-1873.
41. Parr RG, Pearson RG (1983) Absolute hardness: companion parameter to absolute electronegativity. J Am Chem Soc 105: 7512.
42. Pauling L(1960) The Nature of the Chemical Bond, Coruell University Press, Ithaca, New York, USA.
43. Parr RG, Yang W (1989) Density-Functional Theory of Atoms and Molecules, Oxford University Press, New York, USA.

44. Ayers PW, Parr RG (2000) Variational Principles for Describing Chemical Reactions: The Fukui Function and Chemical Hardness Revisited. J Am Chem Soc 122: 2010-2018.

45. Lehr GF, Lawler RG (1984) Quantitative CIDNP evidence for the SH2 reaction of alkyl radicals with Grignard reagents. Implication to the iron catalyzed Kharasch reaction. J Am Chem Soc 106: 4048-4049.

46. Nendel M, Houk KN, Tolbert L M, Vogel E, Jiao H (1998) Bond Alternation and Aromatic Character in Cyclic Polyenes:Assessment of Theoretical Methods for Computing the Structures and Energies of Bismethano[14] annulenes. J Phys Chem 102: 7191

47. Choi CH, Kertesz M (1998) Bond length alternation and aromaticity in large annulenes. Journal of Chemical Physics 108: 6681.

48. Vektariene A, Janciene R (2009) The DFT reactivity estimation of amino-1,5-benzodiazepin-2-ones in the ciclization reaction with dimethyl-2-oxoglutaconate. 13th International Electronic Conference on Synthetic Organic Chemistry (ECSOC-13).

49. Bull Korean (2011) Chemical Society 32: 678.

50. Thanthiriwatte KS, Nalin de Silva KM (2002) Non-linear optical properties of novel fluorenyl derivatives—ab initio quantum chemical calculations. Journal of Molecular Structure (Theochem) 617: 169.

51. Sun YX, Hao QL, Yu ZX, Wei WX, Lu LD, et al. (2009) Experimental and density functional studies on 4-(4-cyanobenzylideneamino)antipyrine. Molecular Physics 107: 223.

52. Ahmed AB, Feki H, Abid, Y, Boughzala H, Minot C, et al. (2009) Crystal structure, vibrational spectra and theoretical studies of l-histidiniumdihydrogen phosphate-phosphoric acid. J Mol Struct 920: 1.

53. Abraham JP, Sajan D, Shettigar V, Dharmaprakash SM, Nemec I et al., (2009) Efficient π-electron conjugated push-pull nonlinear optical chromophore 1-(4-methoxyphenyl)-3-(3,4-dimethoxyphenyl)-2-propen-1-one: A vibrational spectral study. J Mol Struct 917: 27.

54. Sagdinc SG, Esme A (2010) Theoretical and vibrational studies of 4,5-diphenyl-2-2 oxazole propionic acid (oxaprozin). Spectrochim Acta A Mol Biomol Spectrosc 75: 1370-1376.

55. Ahmed AB, Feki H, Abid Y, Boughzala H, Minot (2010) Crystal studies, vibrational spectra and non-linear optical properties of l-histidine chloride monohydrate C. Spectrochimica Acta Part A 75: 293.

56. Jiang YJ (2012) DFT study on nonlinear optical properties of lithium-doped corannulene. Chinese Science Bulletin 57: 4448-4452.